

# Linear Viscoelasticity of Colloidal Hard Sphere Suspensions near the Glass Transition

T. G. Mason<sup>1,2</sup> and D. A. Weitz<sup>1</sup>

<sup>1</sup>*Exxon Research and Engineering Company, Route 22E, Annandale, New Jersey 08801*

<sup>2</sup>*Department of Physics, Princeton University, Princeton, New Jersey 08544*

(Received 3 April 1995)

The frequency-dependent viscoelastic shear modulus of concentrated suspensions of colloidal hard spheres is shown to be strongly modified as the volume fraction approaches the glass transition. The elastic or storage component,  $G'$ , becomes larger than the viscous or loss component,  $G''$ . The frequency dependence of  $G'$  develops a plateau while that of  $G''$  develops a minimum. We propose a physical model to account for these data, using a description of the glasslike behavior based on mode-coupling theory, and a description of the high-frequency behavior based on hydrodynamic flow calculations.

PACS numbers: 83.50.Fc, 64.70.Pf, 82.70.Dd, 83.70.Hq

Suspensions of solid particles with an interaction potential determined solely by excluded volume, or hard spheres, represent one of the most important classes of colloidal dispersions [1]. Understanding their behavior is an essential first step in understanding more complex suspensions of technological significance. Of particular importance are their rheological properties, as they control the flow behavior as well as the viscosity and the elasticity of the suspension. A key measure of these are the linear viscoelastic moduli which determine the response of the suspension to small oscillatory shears which weakly perturb the equilibrium structure. At low frequencies, shear-induced perturbations are relaxed by Brownian motion; this dissipates energy, and the suspension is predominantly viscous. However, at higher frequencies, the perturbations can no longer be relaxed in the period of the oscillation; the change in the equilibrium configuration results in energy storage and hence in an increase in the elastic component. The characteristic frequency is determined by the ratio of the convection rate due to the shear to the diffusional relaxation rate, or the Peclet number  $Pe = a^2 \dot{\gamma} / D_s$ , where  $a$  is the particle radius,  $\dot{\gamma}$  the shear rate, and  $D_s$  the short-time diffusion coefficient which is dependent on the particle volume fraction,  $\phi$ . The magnitude of the elasticity is set by the temperature,  $k_B T / a^3$ , the only energy density scale in the system. Both the viscosity and the elasticity should diverge as the volume fraction approaches random close packing  $\phi_c \approx 0.64$ , where the packing constraints no longer allow for particle motion. Nevertheless, within this picture, data for the storage and loss moduli for different  $\phi$  and  $T$  should all scale onto a unique pair of curves. Exactly this sort of behavior has been reported in earlier important studies of the linear viscoelasticity of hard spheres [2,3].

While very basic and appealing, this picture neglects an essential feature of hard spheres: their phase behavior. Highly monodisperse particles undergo an entropically driven liquid-solid transition [4], forming structures with long range order at  $\phi \approx 0.49$ . When quenched from a disordered configuration, crowding of the parti-

cles leads to a liquid-glass transition at  $\phi_g \approx 0.56$  [5]. Less monodisperse spheres do not exhibit the ordered solid phase but do form colloidal glasses, albeit with a somewhat different  $\phi_g$  [6]. The liquid-glass transition in hard sphere colloids has been studied extensively with light scattering [7]. However, a colloidal glass is a solid, even though it exists at volume fractions well below random close packing. As a result, the glass transition should have profoundly affected the linear viscoelasticity, but this has never been investigated.

In this Letter we show that the liquid and glass phase behavior of hard spheres dramatically affects their viscoelasticity; as  $\phi$  approaches the colloidal glass transition, the structure of the suspension results in a strongly frequency and volume fraction dependent contribution to both the storage modulus,  $G'(\omega)$ , and the loss modulus,  $G''(\omega)$ . To account for this behavior, we present a physical model that combines a description of the onset of the glass phase using mode-coupling formalism with the high-frequency contribution of Brownian motion. The observed behavior precludes the simple scaling of the data reported previously, and directly probes the effects of the phase behavior.

We used suspensions of uncoated silica spheres in ethylene glycol, which interact as hard spheres [3]. Their polydispersity was about 20%, which prevented crystallization; however, they could form a colloidal glass. Their hydrodynamic radius was measured as  $a = 0.21 \mu\text{m}$ , using dynamic light scattering from a dilute suspension. Measurements of  $G'(\omega)$  and  $G''(\omega)$  were performed with a strain controlled rheometer, using a double wall Couette geometry, and at  $T = 23^\circ\text{C}$ , where the solvent viscosity was  $\eta_0 = 17 \text{ cP}$ . The most concentrated suspension was prepared by centrifugation and had a volume fraction of  $\phi \approx 0.56$ , determined with pycnometric and vacuum desiccation techniques. We lowered  $\phi$  by diluting with pure ethylene glycol supernatant recovered from the centrifugation. Although samples of higher concentration could be obtained by further centrifugation, their very long relaxation times made them impossible to load in the cell, precluding their study.

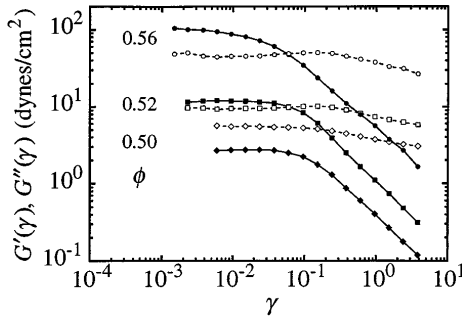


FIG. 1. The dependence of the storage (solid symbols) and loss (open symbols) moduli on the maximum applied strain for several different volume fractions. The measurements are performed at a frequency of 1 rad/s. Note the large increase with  $\phi$  and the dominance of the storage modulus at high  $\phi$ .

Typical results for the storage (closed points) and loss (open points) moduli, as a function of applied strain  $\gamma$  measured at a frequency of  $\omega = 1$  rad/s, are shown in Fig. 1 for several different volume fractions. For sufficiently small strains, both  $G'$  and  $G''$  are independent of  $\gamma$ . We observe a dramatic onset of a dominant storage modulus as  $\phi$  is increased over a very small range. At  $\phi \approx 0.50$ , the loss modulus is larger than the storage modulus, and the suspension is primarily viscous. By contrast, at  $\phi \approx 0.56$ , the storage modulus is larger, and the suspension is dominantly elastic. Furthermore, the strain where the response becomes  $\gamma$  dependent decreases with increasing  $\phi$ . In addition, for the larger  $\phi$ , the apparent loss modulus increases, exceeding the storage modulus at higher  $\gamma$ , indicating that the elastic behavior is limited to low strains. These results underscore the importance of a sufficiently low strain to ensure a linear response.

The frequency dependence of  $G'(\omega)$  and  $G''(\omega)$  for different  $\phi$  is shown in Figs. 2(a) and 2(b), respectively. At the lower  $\phi$ ,  $G''(\omega)$  is dominant, and both moduli increase with frequency. However, as  $\phi$  increases,  $G'(\omega)$  begins to dominate over an extended range of frequencies; moreover, it develops a plateau where it varies only very slowly with frequency, while  $G''(\omega)$  exhibits a definite and reproducible minimum. At higher frequencies, both moduli begin to increase, with  $G''(\omega)$  rising more sharply, ultimately overtaking  $G'(\omega)$ . This behavior is dramatically different from the scaling form previously reported.

To understand the data, we develop a physical model that incorporates the relevant features of the scaling picture, but also includes the consequences of the phase behavior of the hard spheres. We hypothesize that the increase in the elasticity and the plateau behavior of  $G'(\omega)$  reflects the effects of the approach to the colloidal glass transition at  $\phi_g$ . The essential physics that must be included describes the relaxation of density fluctuations of the spheres, which has been probed with light scattering [7]. At very short times, the relaxation of these density

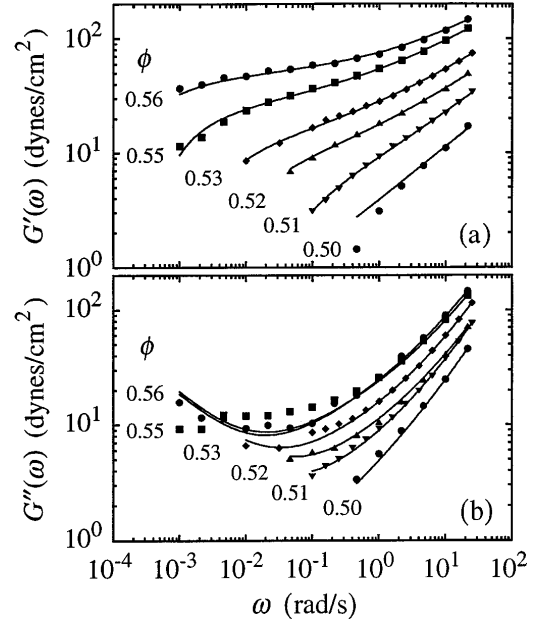


FIG. 2. The frequency dependences of the (a) storage and (b) loss moduli for different volume fractions. All the measurements were performed at sufficiently low strains to be in the linear regime. The solid lines represent the fit to the model discussed in the text.

fluctuations reflects the localized motion of the individual spheres, entailing the full details of the hydrodynamic interactions. However, at longer times particles are trapped in cages formed by their neighbors. Below  $\phi_g$ , the cages slowly break up, making the system ergodic. By contrast, above  $\phi_g$ , the cages cannot break up, and the system is nonergodic. Changes in the configuration of these cages provides a mechanism for energy storage and dissipation, contributing to the moduli; the evolution of these cages determines the frequency dependence. This sort of particle dynamics is observed in these samples with diffusing wave spectroscopy [8].

To describe the cage dynamics, we use the formalism of mode-coupling theory [9,10], which describes light scattering data from hard spheres near  $\phi_g$  [7]. Within mode-coupling theory, the cage dynamics are described by the  $\beta$  decay. We take advantage of a feature predicted by mode-coupling theory near  $\phi_g$ : The temporal autocorrelation functions of all variables coupled to density fluctuations are identical in form. Thus we assume that the stress autocorrelation function has the same functional form as the density autocorrelation function that accounts for the light scattering data, and use the generic, asymptotic mode-coupling form for the  $\beta$  regime on the liquid side of  $\phi_g$  [7,9],

$$C_{\tau\tau}(t) = f_{\tau\tau}^C + h_{\tau\tau} c_{\sigma} \left[ \left( \frac{t}{t_{\sigma}} \right)^{-a'} - B \left( \frac{t}{t_{\sigma}} \right)^{b'} \right]. \quad (1)$$

Here the mode-coupling parameters include the nonergodicity parameter,  $f_{\tau\tau}^C$ , the critical amplitude and scale,  $h_{\tau\tau}$

and  $c_\sigma$ , and the  $\beta$ -scaling time,  $t_\sigma$ . Mode-coupling theory places significant constraints on the behavior of these parameters; it predicts that  $f_{\tau\tau}^c$  and  $h_{\tau\tau}$  are  $\phi$  independent, while  $c_\sigma \sim \sigma^{1/2}$  and  $t_\sigma \sim \sigma^{1/(2a')}$ , where the separation parameter is  $\sigma = (\phi_g - \phi)/\phi_g$ . It also predicts  $a' = 0.301$ ,  $b' = 0.545$ , and  $B = 0.963$  for hard spheres [9]. The near-glass contribution to the complex shear modulus is given by  $G_g^*(\omega) = G_0[i\omega C_{\tau\tau}^*(\omega)]$ , where  $C_{\tau\tau}^*(\omega)$  is the unilateral complex Fourier transform of the stress autocorrelation function, and  $G_0$  is the thermodynamic derivative of the stress with respect to the strain, which sets the scale of the stress relaxation. The real and imaginary parts of  $G_g^*(\omega)$  contribute to the storage and loss moduli, respectively.

The high-frequency behavior is not described within mode-coupling formalism. Instead, we incorporate the effects of energy storage due to Brownian motion by using the form calculated for a diffusional boundary layer; this ignores lubrication effects, which will ultimately cause  $G'$  to reach a constant plateau as  $\omega$  increases [11]. Since our highest normalized frequencies are large,  $\omega a^2/D_s \sim 10^1 - 10^2$ , we consider only the high-frequency asymptotic form predicted by flow calculations [11] and by kinetic theory [12],

$$G_D'(\omega) = \frac{3}{5\pi} \frac{k_B T}{a^3} \phi^2 g(2a, \phi) [\omega \tau_D]^{1/2}, \quad (2)$$

where  $\tau_D = a^2/D_s$  is the diffusional time determined by the  $\phi$ -dependent short-time diffusion coefficient. For these high volume fractions, we approximate the radial pair distribution function at contact by  $g(2a, \phi) = 0.78/(0.64 - \phi)$ , consistent with computer simulations that indicate a divergence at random close packing [1,13]. Physically,  $G_D'(\omega)$  reflects the additional driving force for diffusional motion that arises from the hard sphere interaction potential, which prevents the particles from touching when the shear makes them approach their neighbors. Because of causality, the Kramers-Kronig relations require a similar contribution to the loss modulus,  $G_D''(\omega) = G_D'(\omega)$ . We must also include the contribution of the high-frequency suspension viscosity,  $G_S''(\omega) = \eta_\infty \omega$ .

To obtain the complete elastic modulus, we sum the individual contributions; this implicitly assumes that the individual stress autocorrelation functions are statistically independent, reflecting their significantly different frequencies. We obtain

$$G'(\omega) = G_P + G_\sigma \left[ \Gamma(1 - a') \cos\left(\frac{\pi a'}{2}\right) (\omega t_\sigma)^{a'} - B \Gamma(1 + b') \cos\left(\frac{\pi b'}{2}\right) (\omega t_\sigma)^{-b'} \right] + G_D'(\omega), \quad (3)$$

$$G''(\omega) = G_\sigma \left[ \Gamma(1 - a') \sin\left(\frac{\pi a'}{2}\right) (\omega t_\sigma)^{a'} + B \Gamma(1 + b') \sin\left(\frac{\pi b'}{2}\right) (\omega t_\sigma)^{-b'} \right] + G_D''(\omega) + \eta_\infty \omega, \quad (4)$$

where  $\Gamma$  is the gamma function. The plateau modulus,  $G_P = G_0 f_{\tau\tau}^c$ , contributes only to  $G'(\omega)$  and represents the overall magnitude of the near-glass elasticity. Moreover, as expected from the mode-coupling description, the storage modulus has an inflection point at the plateau value, while the loss modulus has a minimum; the frequency of these is set by  $1/t_\sigma$ . The viscoelastic amplitude,  $G_\sigma = G_0 h_{\tau\tau} c_\sigma$ , determines the degree of variation of  $G'(\omega)$  about its plateau value and the magnitude of  $G''(\omega)$  at the minimum. To compare this model with our data, we simultaneously fit both  $G'(\omega)$  and  $G''(\omega)$  by Eqs. (3) and (4) for each volume fraction, using  $G_P$ ,  $G_\sigma$ ,  $t_\sigma$ ,  $D_s$ , and  $\eta_\infty$  as fitting parameters. As shown by the solid lines in Fig. 2, excellent agreement is obtained for virtually all of the data; in particular, this model captures correctly the plateau behavior observed in  $G'(\omega)$ .

Although our model provides an excellent description of the form of the data, it does possess many fitting parameters. Thus an additional critical test of its validity is the  $\phi$  dependence of these parameters; the physics of the diffusional boundary layer and mode-coupling theory places severe constraints on their behavior. The high-frequency behavior is dominated by  $\eta_\infty$  and  $D_s$ ; in fact, the data cannot be adequately fit without including their contribution. However, their  $\phi$  dependence is known independently from theoretical predictions and experimental measurements of the viscosity and self-diffusion coefficients. In Fig. 3(a), we plot  $\eta_0/\eta_\infty$  (open points) and  $D_s/D_0$  (solid points) as functions of  $\phi$ ,

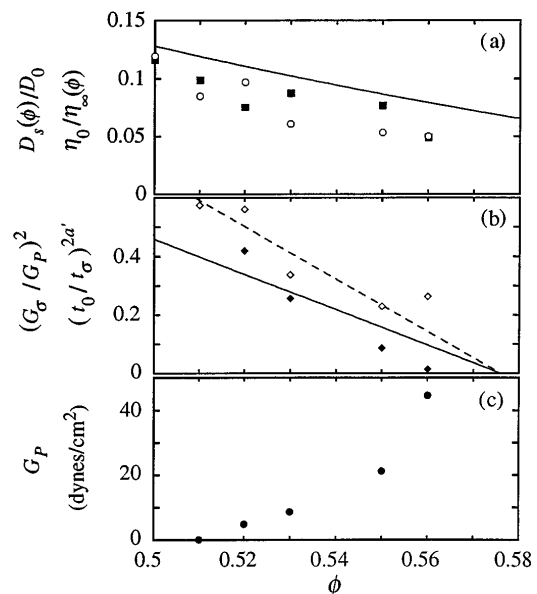


FIG. 3. The  $\phi$  dependence of the parameters obtained by the fit to the model. (a)  $\eta_0/\eta_\infty$  (open circles) and  $D_s/D_0$  (solid squares); the solid line is a published prediction of the viscosity [15]. (b)  $(G_\sigma/G_P)^2$  (solid diamonds) and  $(t_0/t_\sigma)^{2a'}$  (open diamonds), where  $t_0 = 2\pi$  sec, with fits to the linear dependence expected from mode-coupling theory, giving  $\phi_g \approx 0.58$ . (c) The plateau modulus  $G_P$ .

where  $D_0 = k_B T / 6\pi\eta_0 a$ . They are nearly identical, as expected over this range of  $\phi$  [14]; moreover, they are consistent with independent measurements and computer simulations for  $\eta_0/\eta_\infty$  [15], as shown by the solid line. Thus we conclude that the contributions of the diffusional boundary layer and the suspension viscosity included in our model correctly describe the high-frequency behavior of the data.

The remaining three parameters reflect the contribution of the mode-coupling theory to the viscoelastic modulus and thus should be subject to the constraints of its predictions. At the lowest volume fraction, the contribution of the near-glass modulus is negligible. However, at the higher volume fractions, we find that both  $G_P$  and  $G_\sigma$  increase dramatically with  $\phi$ . Nevertheless, mode-coupling theory predicts that the  $\phi$  dependence of their ratio is determined by  $(G_\sigma/G_P)^2 \sim c_\sigma^2 \sim \sigma$ , and thus should go linearly to zero as  $\phi$  approaches  $\phi_g$ . This is indeed observed, as shown in Fig. 3(b), where we plot the  $\phi$  dependence of  $(G_0/G_P)^2$  with solid points. Furthermore, mode-coupling theory predicts that  $t_\sigma^{-2a'} \sim \sigma$  below the glass transition. Thus in Fig. 3(b), we plot with open points the  $\phi$  dependence of  $(t_0/t_\sigma)^{-2a'}$ , where we have taken  $t_0 = 2\pi$  sec for convenience; again, the predicted linear decrease is observed. These data are consistent with  $\phi_g \approx 0.58$ , as shown by the solid lines which are fits with the value of  $\phi_g$  constrained to be the same for each parameter. We emphasize, however, that uncertainty in the fitting parameters, and in our knowledge of the exact volume fraction, preclude a precise determination of  $\phi_g$  and comparison to other systems. Nevertheless, these results support our hypothesis that the low-frequency behavior of the viscoelastic moduli reflect the approach to glass transition and are correctly modeled by the predictions of mode-coupling theory.

Finally, we also show in Fig. 3(c) the  $\phi$  dependence of the plateau modulus,  $G_P = G_0 f_{\tau\tau}^c$ . It displays the expected behavior; it goes to zero as  $\phi$  decreases, and diverges with increasing  $\phi$ . We expect  $G_P$  to depend on the amount of free volume in the system. Thus it should diverge at  $\phi_c$  rather than  $\phi_g$ , but unfortunately the experimental uncertainty in  $\phi_g$  precludes an accurate assessment of this. We note, however, that the decrease in the maximum  $\gamma$  for linear moduli exhibited in Fig. 1 suggests a vanishing free volume. There is one theoretical suggestion that the zero frequency modulus above the glass transition should depend on the derivative of the radial distribution function,  $dg(r, \phi)/dr$ , evaluated at contact,  $r = 2a$  [16]. This prediction might also be expected to account for  $G_0$  near  $\phi_g$ ; however, the  $\phi$  dependence of this derivative is not known.

Our data strongly suggest that the phase behavior of hard spheres has a pronounced effect on their viscoelasticity, which is dramatically modified as the glass transition

is approached. Moreover, they show that a single parameter,  $Pe$ , is not sufficient to scale the data for all  $\phi$  and  $T$ . The temperature dependence of  $G_D'$  and  $G_D''$  should depend primarily on that of  $\eta_\infty$  which controls  $D_s$  and hence that time scale, consistent with the simple scaling. By contrast, the contribution of the near-glass structure depends on the relaxation of cages having much larger length scales, and this could conceivably have a very different temperature dependence. This may account for why the behavior reported here was not observed in previous experiments [2,3], which investigated the viscoelastic behavior at higher frequencies or lower temperatures. Finally, while our physical model provides an excellent account of the data, it is nonetheless a phenomenological model, since the mode-coupling contribution is based on an analogy to the density correlation function. Thus these data do not constitute a test of mode-coupling theory. Nevertheless, the success of our model will, we hope, provide the impetus for more microscopic calculations of the shear viscoelasticity predicted by mode-coupling theory for hard sphere suspensions. This would then provide an important additional test of the validity of the theory.

We have benefited from discussions with Herman Cummins, Wolfgang Götze, Bill Russel, Rudy Klein, and Scott Milner. This work was supported in part by NASA.

- 
- [1] W.B. Russel, D.A. Saville, and W.R. Schowalter, *Colloidal Dispersions* (Cambridge University, Cambridge, 1989).
  - [2] J.C. van der Werff, C.G. de Kruif, C. Blom, and J. Mellema, Phys. Rev. A **39**, 795 (1989).
  - [3] T. Shikata and D.S. Pearson, J. Rheol. **38**, 601 (1994).
  - [4] P.N. Pusey and W. van Megen, Nature (London) **320**, 340 (1986).
  - [5] P.N. Pusey and W. van Megen, Phys. Rev. Lett. **59**, 2083 (1987).
  - [6] E. Bartsch, M. Antonietti, W. Schupp, and H. Sillescu, J. Phys. Chem. **97**, 3950 (1992).
  - [7] W. van Megen and S.M. Underwood, Phys. Rev. E **49**, 4206 (1994).
  - [8] T.G. Mason and D.A. Weitz, Phys. Rev. Lett. **74**, 1250 (1995).
  - [9] W. Götze and L. Sjogren, Rep. Prog. Phys. **55**, 241 (1992).
  - [10] H.Z. Cummins, G. Li, W.M. Du, and J. Hernandez, Physica (Amsterdam) **204A**, 169 (1994).
  - [11] R.A. Lionberger and W.B. Russel, J. Rheol. **38**, 1885 (1994).
  - [12] I.M. de Schepper, H.E. Smorenburg, and E.G.D. Cohen, Phys. Rev. Lett. **70**, 2178 (1993).
  - [13] L.V. Woodcock, Ann. N.Y. Acad. Sci. **371**, 274 (1981).
  - [14] E.G.D. Cohen and I.M. de Schepper (private communication).
  - [15] A.J.C. Ladd, J. Phys. Chem. **93**, 3484 (1990).
  - [16] J.F. Brady, J. Phys. Chem. **99**, 567 (1993).